jove

Venous Thrombosis Assay in a Mouse Model of Cancer

Saran Lotfollahzadeh[1], **Xiaosheng Yang**[1], **David Jasen Wu Wong**[1], **Jingyan Han**[2], **Francesca Seta**[2], **Suvranu Ganguli**[3], **Asha Jose**[1], **Katya Ravid**[4,5], **Vipul C. Chitalia**[1,6,7,8]

[1] Renal Section, Department of Medicine, Chobanian and Avedisian School of Medicine, Boston University [2] Vascular Biology Section, Department of Medicine, Chobanian and Avedisian School of Medicine, Boston University [3] Division of Interventional Radiology, Department of Radiology, Chobanian and Avedisian School of Medicine, Boston University [4] Department of Medicine, Whitaker Cardiovascular Institute, Chobanian and Avedisian School of Medicine, Boston University [5] Department of Biochemistry and Cell Biology, Chobanian and Avedisian School of Medicine, Boston University [6] Veterans Affairs Boston Healthcare System [7] Institute of Medical Engineering and Sciences, Massachusetts Institute of Technology [8] Center of Cross-Organ Vascular Pathology, Department of Medicine, Chobanian and Avedisian School of Medicine, Boston University

Corresponding Authors

Katya Ravid
kravid@bu.edu

Vipul C. Chitalia
vichital@bu.edu

Citation

Lotfollahzadeh, S., Yang, X., Wu Wong, D.J., Han, J., Seta, F., Ganguli, S., Jose, A., Ravid, K., Chitalia, V.C. Venous Thrombosis Assay in a Mouse Model of Cancer. *J. Vis. Exp.* (203), e65518, doi:10.3791/65518 (2024).

Date Published

January 5, 2024

DOI

10.3791/65518

URL

jove.com/video/65518

Abstract

This methodology paper highlights the surgical nuances of a rodent model of venous thrombosis, specifically in the context of cancer-associated thrombosis (CAT). Deep venous thrombosis is a common complication in cancer survivors and can be potentially fatal. The current murine venous thrombosis models typically involve a complete or partial mechanical occlusion of the inferior vena cava (IVC) using a suture. This procedure induces a total or partial stasis of blood and endothelial damage, triggering thrombogenesis. The current models have limitations such as higher variability in clot weights, significant mortality rate, and prolonged learning curve. This report introduces surgical refinements using vascular clips to address some of these limitations. Using a syngeneic colon cancer xenograft mouse model, we employed customized vascular clips to ligate the infrarenal vena cava. These clips allow residual lip space similar to a 5-0 polypropylene suture after IVC ligations. Mice with the suture method served as controls. The vascular clip method resulted in a consistent reproducible partial vascular occlusion and greater clot weights with less variability than the suture method. The larger clot weights, greater clot mass, and clot to the IVC luminal surface area were expected due to the higher pressure profile of the vascular clips compared to a 6-0 polypropylene suture. The approach was validated by gray scale ultrasonography, which revealed consistently greater clot mass in the infrarenal vena cava with vascular clips compared to the suture method. These observations were further substantiated with the immunofluorescence staining. This study offers an improved method to generate a venous thrombosis model in mice, which can be employed to deepen the mechanistic understanding of CAT and in translational research such as drug discovery.

Copyright © 2024 JoVE Journal of Visualized Experiments

Introduction

Cancer-associated venous thromboembolism (VTE)

Venous thromboembolism (VTE) risk is 4 to 7 times higher in cancer survivors compared to the general population[1,2,3]. This condition proves fatal in one out of seven patients with cancer. The incidence of VTE varies depending on the type of cancer and the tumor burden and is highest among patients with pancreatic and gastric cancers[4].

Cancer-associated VTE in cancer patients has prognostic significance. It is associated with unfavorable overall survival in the first year after a cancer diagnosis, even after adjusting for age, race, and stage of underlying cancer[5]. These findings highlight the importance of examining cancer associated VTE and the need to probe its mechanism using an animal model. The translational relevance of this area is further emphasized by the fact that VTE in cancer patients is preventable and treatable with thromboprophylaxis and antithrombotic therapy[6].

Animal models of cancer and venous thrombosis

Cancer models are conventionally termed xenografts, which entail the injection of cancer cells in mice. The injection of cancer cells at a site like its origin is referred to as an orthotopic model, while at a different site (subcutaneous plane over the flank) is known as a heterotopic model. The species of origin of cancer cells determines them as an allogeneic model, such as the HT-29 cell line (human colon cancer)[7,8,9]. On the contrary, syngeneic models use the murine cancer cell lines, including RenCa and MC-38 cell lines[3,10].

The literature has described arterial, venous, and capillary thrombosis models in rodents. Venous thrombosis is induced in the inferior vena cava (IVC) by mechanical injury (guide wire) or complete IVC ligation, chemical (Ferric chloride), or electrolytic injury. Ferric chloride-induced thrombosis or IVC ligation represents complete occlusion models. The latter results in the stasis of blood and inflammatory infiltrates in veins[11,12,13]. The complete ligation model results in a high rate of thrombosis formation in 95% to 100% of mice. The partial IVC ligation model might include interruption of lateral iliolumbar branches, and the venous return is abrogated by applying suture ligations in the distal target points of IVC[12]. Sometimes, a space holder is used to interrupt the venous return partially. However, the thrombus weight is inconsistent in the current partial occlusion model, resulting in high variability in clot weights and heights[12,14].

Both these large vein mechanical models (partial and complete) have limitations. First, IVC ligation (stasis model) often results in hypotension. The blood gets shunted through vertebral veins. Though in experienced hands, the mortality with this model ranges from 5%-30%, with the higher rate expected during the learning curve. Importantly, the complete occlusion model does not reproduce deep vein thrombosis (DVT) in humans, where a thrombus typically is nonocclusive. Complete occlusion is likely to alter hemorheological factors and pharmacodynamic parameters, altering the bioavailability of compounds at the local site. Due to these limitations, complete occlusion models may not be optimal for testing novel chemical compounds for therapeutic purposes and drug discoveries[12].

It should be noted that to provide a more clinically relevant murine model of venous thrombosis with decreased flow with endothelial damage, a venous thrombosis model has been introduced, where DVT is triggered by the restriction

Copyright © 2024 JoVE Journal of Visualized Experiments

of blood flow in the absence of endothelial disruption. The model was validated by scanning electron microscopy[15]. A preferred clinically relevant thrombosis model is one with near complete thrombosis that enables drug discoveries. The clot formation in the current partial occlusion models is inconsistent, resulting in high variability in the clot weight and heights[12,16]. Furthermore, the clot weight is variable with the conventional methods, requiring more mice per studies[12].

Previous cancer-associated thrombosis models focused on colon, pancreatic, and lung cancer and were all complete occlusion models[17,18,19]. This manuscript modifies the partial occlusion thrombosis model to provide clots with lower variability and mouse mortality **(Figure 1)**. Former studies used allogeneic cancer cell lines on immunocompromised athymic mice background[19,20,21]. This manuscript uses an MC-38 cell syngeneic xenograft in C57Bl6/J mice, which allows the use of immunocompetent mice and examination of immune components to thrombogenesis.

Protocol

For this study, 16 female C57Bl6/J mice, 8-12 weeks in age, and a body weight of 20 to 25 g were used. The mice were housed under standard conditions and were fed with chow and water *ad libitum*. This study was performed with the approval of the Institutional Animal Care and Use Committee (IACUC) at Boston University. The open procedures described here were undertaken in a sterile condition.

1. Xenograft model

1. Cell culture

    1. Prior to heterotopic subcutaneous implantation, grow MC-38 cells as a monolayer to 80% confluency.

    2. Following trypsinization and resuspension in 10% FBS-containing media, centrifuge cells at 277 x *g*, 4 °C for 5 min. Then, resuspend the cells in serum-free media to a concentration of 1 x 10^4 MC-38 cells/µL serum-free media.

        1. For trypsinization, culture the MC-38 cells until they reach a desired confluence (usually around 70%-80%) and then aspirate the culture medium from the Petri dish.

        2. Add 1 mL of trypsin-EDTA solution and incubate the cells with trypsin for 1 min at 37 °C to allow detachment. Gently tap or shake the Petri dish to ensure even detachment.

        3. Add a culture medium containing serum or a trypsin inhibitor to neutralize the activity and prevent further cell dissociation. Collect the detached cells along with the neutralized trypsin solution.

        4. For resuspension, once the cells are detached through trypsinization, prepare them for transplantation or further experiments. Centrifuge the collected cell suspension at 277 x *g* to pellet the cells.

        5. Carefully remove the supernatant (liquid above the cell pellet). Add 9 mL of culture medium, buffer, or solution to the cell pellet to achieve the desired cell concentration for transplantation or experimentation.

Copyright © 2024 JoVE Journal of Visualized Experiments

6. Gently resuspend the cells by pipetting up and down or using a culture flask shaker. Avoid vigorous pipetting that could damage the cells.
   NOTE: Depending on the variant or cell line used, cells can be resuspended in a 1:1 ratio of solubilized basement membrane matrix and serum-free media to slow highly aggressive mouse cell growth and dissemination after implantation. All cell culture steps should be undertaken in a complete aseptic hood in a cell culture specifically allocated space and were tested for mycoplasma regularly.

3. Count the cells with an automated cell counter as per the provided manual protocol.

2. Cell implantation

1. Randomly assign eight mice to the experimental group, and eight mice to the control group as follows. In the control group, use mice with MC38 xenograft and perform IVC ligation with a polypropylene 5-0 suture. In the experimental group, use mice with MC38 xenograft and perform IVC ligation with a customized vascular clip.

2. Place the mouse in left lateral recumbency and shave the right side between the forelimbs and hindlimbs. Apply alcohol and iodine along the dorsal lumbar area to aseptically prepare the area for injection.

3. Inject 2 x 10^6 MC-38 cells prepared in 200 µL of medium subcutaneously in the flank, halfway between the animal's most distal rib and pelvic eminence using a 27G needle while holding the animal gently in the non-dominant hand.

4. Following injection, inspect the animals carefully and put them back into the cage. The animals should be inspected for the followings; 1. Changes in behavior, activity levels, and overall mobility of the mice. Any significant changes could indicate discomfort or health issues. 2. The overall physical condition of the mice, including fur quality, grooming habits, and any visible signs of distress or abnormalities 3. Return to food consumption and water intake 4. Any changes in their activity level, posture, or interactions with cage mates. Lethargy or increased aggression could be signs of distress.

2. Follow-up of tumor growth

1. Monitor the animals on a bi-weekly basis for tumor growth trends for 3-4 weeks. Measure the tumors with a caliper and record the tumor dimensions.

1. Measure the tumors along their longest axis (L) and the axis perpendicular to the long axis (W). Calculate the tumor volume (V) using the equation L x (W^2) = V. If the tumor size surpasses 20 mm in each dimension and or the tumor has evidence of ulceration, euthanize the animals before the termination of the experiment.

2. Once the tumor volume reaches 400 mm^3, plan to use the mice for IVC ligation.

3. Anesthesia and preparation

1. Anesthetize the mouse in an isoflurane chamber and inject the analgesic subcutaneously: Hold the animal from the base of the tail. Keep the animal on the dorsum surface of the non-dominant hand.

2. Transfer the animal to the continuous anesthetic induction chamber filled with 3%-4% isoflurane. Confirm adequate general anesthesia with the absence of a toe-pinch reflex. Use a maintenance dose of 1%-3% isoflurane. Apply vet ointment on both eyes.
3. Subcutaneous injection with buprenorphine (opioid for mitigating pain): Dissolve the stock of buprenorphine at a concentration of 0.3 mg/mL in 0.9% sodium chloride (NaCl) to achieve the concentration of 0.03 mg/mL.
4. Inject a dosage of 0.05-0.1 mg/kg of 0.03 mg/mL buprenorphine together with 500 µL of sterile 0.9% NaCl subcutaneously before surgery. In a 20 g mouse amount of 2 µg or 66 µL of 0.03 mg/mL buprenorphine is required.
5. Skin preparation: Place the fully anesthetized mouse in a supine position over the heating blanket. Disinfect the anterior abdominal area with 0.5% chlorhexidine tincture, 2x. Frequently check the temperature of the heating blanket during the procedure and make sure that the temperature does not fall.

4. IVC ligation

1. Midline laparotomy
    1. Incise the abdominal skin with fine scissors starting from xiphoidal eminence to the bladder. Pinch the peritoneum halfway along the skin incision with atraumatic forceps. Ensure adequate space between the incision and the overlying intestines (**Figure 2A**).
    2. Open the peritoneum in a longitudinal manner along with avascular linea alba.
2. Exteriorizing the intestines to the right abdominal side
    1. Pull the intestines with wet cotton tips. Cover the intestines in a completely moist sterile gauze. Ensure that the covered intestines are in a traction-free direction without any excessive traction on the mesenteric vessels.
3. Full exposure of the IVC and branches, including the confluence of the left renal vein to the IVC (**Figure 2B**).
    1. Drop 200-300 µL of normal saline. Explore the ureters', IVC, Aorta, and renal veins course (**Figure 2**).
4. Avascular plane at the confluence point of the infra-renal IVC and the left renal vein confluence.
    1. Pass the polypropylene 6-0 suture through the avascular plane gently 2x-3x with caudal to cephalad movements with the closed tip atraumatic forceps.
    2. Ensure that any minimal oozing is controlled with gentle pressure provided with a cotton tip tamponade. Widen the provided plane by passing the 6-0 polypropylene suture with gentle caudal to cranial movements.
5. Cauterizing the gonadal and lumbar branches (**Figure 2D**)
    1. Up to 4 posterior or lumbar branches might be present. To avoid potential complications of spinal ischemia and claudication, leave the lumbar branches intact in the current protocol.
    2. Check that 2 to 3 side branches, including the bilateral uterine horn arterial supply and hypogastric vessels are present. Ensure consistent disruption of the first bilaterally present branches. Cauterize the bilateral branches just distal to the confluence of the left renal vein and IVC (infra-renal IVC). Ensure that

Copyright © 2024 JoVE Journal of Visualized Experiments

the venous draining vessels of the uterine horn are not disrupted.

NOTE: Side-branch cauterization is opted for because this method provides a smooth and uninterrupted surface, reducing any potential for uncontrolled bleeding. Moreover, cauterization is faster and more feasible than suture ligation with 10-0 sutures. Therefore, the animals will be exposed to a shorter and safer procedure.

6. Double-check the ureters' course and the vasculature to ensure the absence of any oozing or inadvertent cauterizing (**Figure 2C**).

7. IVC ligation with vascular clips in the experimental group

    1. Customize the vascular clips with a width of 2-0 nylon suture by atraumatic forceps. Apply the customized vascular clips in the experimental group circumferentially around the infrarenal IVC.

    2. Apply the vascular clips over the suture. The primary suture passage provides a sufficient avascular plane with two to three meticulous caudal to cranial movements (**Figure 2E-F**).

    3. Further pass the vascular clips through the prepared plane. Prepare the plane at the confluence of the left renal vein and IVC wide enough to allow an uneventful clip passage (**Figure 2E**).

    4. Place the customized vascular clip horizontally, perpendicular to the IVC course, through the prepared plane. Place the vascular clips over the 5-0 polypropylene suture to ensure adequate remaining space (**Figure 2G**).

    5. Ensure that the above steps are performed gently to prevent any vessel damage or bleeding at the site of vascular clips. Observe the surgical field for potential oozing. Apply gentle pressure with the cotton tip to the surgical field in case of oozing.

8. IVC Ligation with suture in the control group

    1. Suture ligation with 6-0 polypropylene suture. Make a surgical square knot suture around the infra-renal IVC in the prepared plane over a 5-0 silk suture.

    2. Once the suture is complete, gently remove the silk suture to ensure adequate remnant space.

9. Perform subcutaneous injection of 200 µL of normal saline.

    NOTE: To provide a comparable technique for partial IVC occlusion with clamp application, the vascular clip is customized in the current study to provide space in between lips. The vascular clip is then placed in the prepared avascular plane in the confluence of the left renal vein and IVC.

10. Close the laparotomy with continuous running 4-0 vicryl suture.

5. Follow-up after the index surgery

1. Monitor the animal continuously post-operation for 1 h or until balance and righting capability are recovered, whatever comes first in an isolated clean cage until fully recovered.

2. Monitor the animal daily for 2 days. If the animal looks distressed, monitor it twice a day for 2 days. Administer postoperative analgesia and fluids per protocol.

    1. Dissolve the stock of buprenorphine with a concentration of 0.3 mg/mL in 0.9% sodium chloride (NaCl) to achieve the concentration of 0.03 mg/mL.

    2. Inject a dosage of 0.05-0.1 mg/kg of 0.03 mg/mL buprenorphine subcutaneously together with 500 µL

of sterile 0.9% NaCl, every 8 to 12 h during the first 48 h following the index surgery. In a 20 g mouse, 2 µg or 66 µL of 0.03 mg/mL buprenorphine would be required.

6. Euthanasia and harvesting the IVC containing the clot

1. Anesthetize the mouse in an isoflurane chamber, hold the animal from the base of the tail and keep the animal on the dorsum surface of your hand.
2. Transfer the animal to the continuous anesthetic induction chamber filled with 3%-4% isoflurane. Place the animal in the supine position.
3. Perform a long midline laparotomy starting from the xiphoid to the bladder as described.
4. Exteriorize the intestine to the right side of the abdomen and harvest the clamped IVC distal to the iliac bifurcation to the extent of infra-renal IVC (**Figure 2G**).
5. Following the clot and tumor harvest, euthanize the animal with cervical dislocation.

7. Statistical analysis

1. Present statistical analysis as the mean, median, and standard deviation (SD) or standard error of the mean (SEM), 25th or 75th percentile, or the entire range of values, including minimum and maximum values, as appropriate. Perform a Student t-test, and the F-test as appropriate. Assess statistical significance at the $p < 0.05$ level.

Representative Results

A group of female C57Bl6/J mice, 8-12 weeks of age, were injected with MC-38 cells at the logarithmic phase of the cell growth. The xenografts grew rapidly between the third- and fourth -weeks post-injection[18]. Once the tumors reached an average volume of 400 mm^3, mice were randomized to the control and experimental groups. The control group underwent IVC ligation with suture, while the experimental mice were subjected to IVC ligation with vascular clip application. The tumor volumes in the control and experimental groups were comparable without significant differences (353 ± 100 mm^3 vs. 367 ± 46.2 mm^3, $p = 0.445$). Infra-renal IVCs to the iliac veins' bifurcation point containing the clot were harvested after 48 h, and the clot weights served as the biological readout of venous thrombogenicity. The postoperative course in all animals in control and experimental groups was uneventful, without evidence of uterine horn discoloration, musculoskeletal ischemia, or claudication issues in the lower limb. During the second laparotomy, no vascular clip displacement was observed. No mortality was observed before the termination of the experiments.

Clot weight to normalized body weight ratio

As mice with xenograft are likely to lose body weight, clots weights (in mg) were normalized to total body weights at the time of harvest (both in mg). Close to a 1.5-fold increase in the normalized clot-to-body weights were observed in mice in the experimental group (mean ± SEM, 0.002580 ± 0.00098) compared with control mice (0.001453 ± 0.002666, P-value: 0.0019; **Figure 3**).

Immunofluorescence assay

The histopathological evaluation was used to examine the IVC and clots. The paraffin-embedded sections from infrarenal vena cava were stained with anti-CD31 (a marker of endothelial cells)[20] and anti-fibrin, and DAPI (**Figure 4A**).

The infrarenal vena cava from control mice showed intact CD31 staining and fibrin partially occupying the vessel's lumen. In the experimental group, CD31 expression was not intact, suggesting endothelial cell damage and a large clot with prominent fibrin expression. The vessel wall also expressed fibrin staining (**Figure 4A**).

For Immunofluorescence, fibrin mouse monoclonal antibody was used at 1:1000 dilution and incubated overnight at 4 °C. For CD31, a rabbit polyclonal anti-CD31 antibody validated for immunoblots and IF (1:1000 and 1:100 overnight at 4 °C) was used. This antibody is known to react against mouse, human, and pig CD31. For IF, the secondary antibodies consisted of Alex Fluor 488, 594, and 647 at 1:250 dilution for 45 min at room temperature.

For image quantification, the entire slide was scanned by a motorized stage system. The images were processed in ImageJ, where the signal was converted to grayscale, and the number and intensity of pixels were analyzed as integrated density. The area of the vein was marked as the region of interest. The integrated density of all the images was normalized to its area[18].

These are shown to be upregulated in models of cancer-associated deep vein thrombosis. The quantitation of several images was performed using integrated density analysis, as done previously using Image J[18]. The control group had significantly lower fibrin expression compared to the experimental group (p:0.0080; **Figure 4B**; 174 ± 104 vs. 503.5 ± 182.4 mean ± SD). Notably, the variances in the Fibrin expressions were lower in the experimental compared to the control group (F statistics, DFn, Dfd: 3.074, 4, 4).

Grayscale ultrasonography

After 2 days of surgery and just prior to the clot harvest, mice underwent grayscale ultrasonography. Mice in both groups showed clots in the infrarenal vena cava. However, the clots were larger in the mice with vascular clip. Representative ultrasonography images are shown in **Figure 5**. An anechoic region of the vessel suggests a patent lumen and a hyperechoic density in the vessel is indicative of an organized clot. The ligated infrarenal vena cava of a mouse from the control group shows a partial clot demarcated by two yellow arrowheads in **Figure 5A**. In contrast, **Figure 5B** shows a large clot nearly occluding the infrarenal vena cava generated with a vascular clip model (depicted by two yellow arrowheads and marked by white asterisks). Of note, the infrarenal vena cava collapsed in the control group while it was enlarged in the experimental group, consistent with the greater clot burden in the latter group.

Both the assays (ultrasonography and IF) suggest that the experimental group had consistently larger clots than the control group.

Copyright © 2024 JoVE Journal of Visualized Experiments

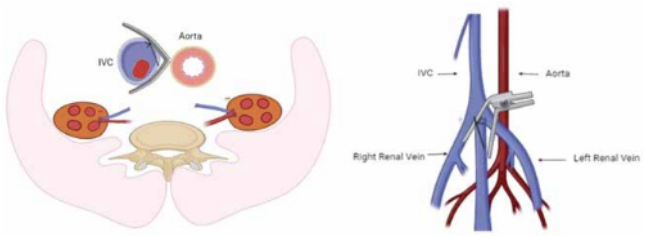

Figure 1: A schematic depicting the IVC-Aorta and the application of the clip over the confluence of the left renal vein (LRV)-IVC. Please click here to view a larger version of this figure.

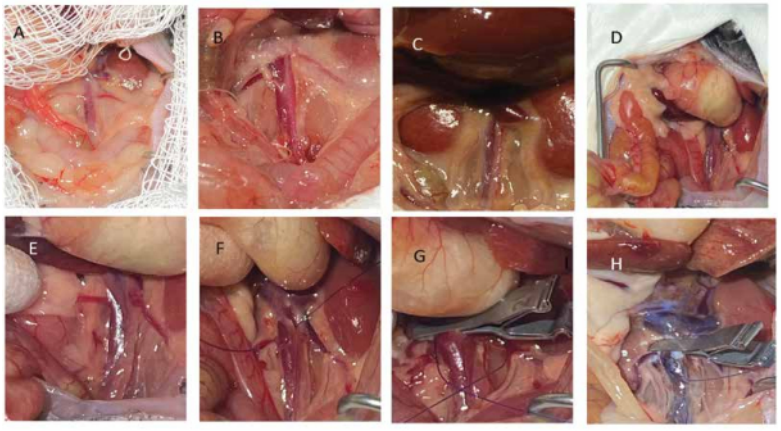

Figure 2: Intraoperative IVC thrombosis model with clips application. (**A**) Midline laparotomy. (**B**) Full exposure of the IVC, including the confluence of the left renal vein to the IVC. (**C**) Demonstrating the ureter course and avoiding any iatrogenic trauma to the left ureter. (**D**) Cauterizing the gonadal branches. (**E**) Dissection of the IVC to the left renal vein confluence point. (**F**) Passing the 5-0 polypropylene suture through the dissected plane to widen the plane for passing the suture. (**G**) Passing a vascular clamp through the prepared plane. (**H**) Clot formation 48 h after the IVC clamping. Please click here to view a larger version of this figure.

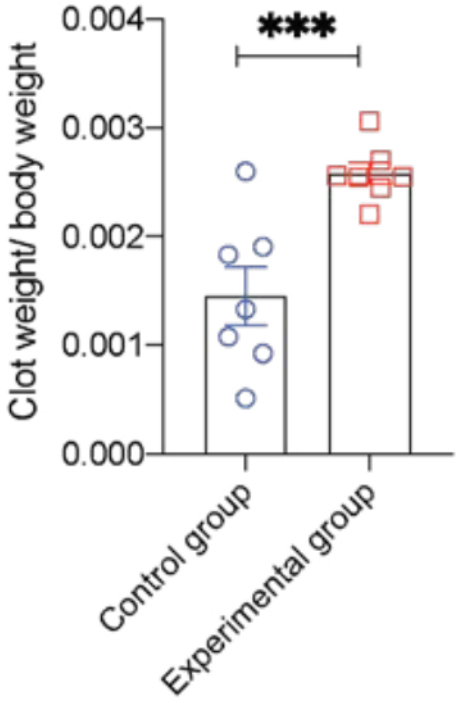

Figure 3: The group of mice with vascular clips IVC ligation, had higher normalized clot-to-body weight ratio.

Average Normalized clot-to-body weight ratio. The unit of both the values expressed in milligram. Error Bars = SD. Student's t-test was applied. P <0.0001 Please click here to view a larger version of this figure.

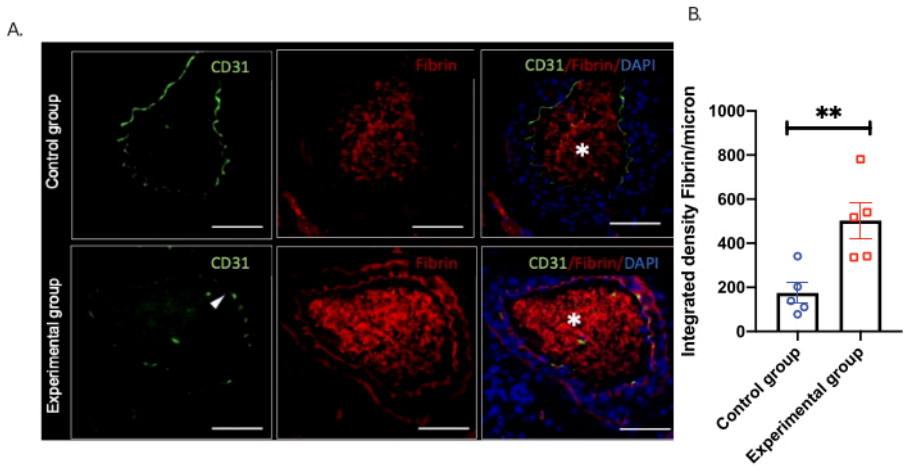

Figure 4: Increased fibrin and CD 31 expression in group of mice with vascular clips IVC ligation. The Representative immunofluorescence images obtained at 100x magnification from the control group with IVC ligation with suture and from the experimental group with IVC ligation with vascular clips. Shown are randomly selected images per mouse (N= 4 mice/ group). (**A**) Fibrin and CD31 expression in the control and experimental groups. Two yellow arrowheads marked by white asterisks depict the large clot nearly occluding IVC, that implies the partially occluded IVC. (**B**) The integrated density of Fibrin: The line represents the median value. Student's T-test was performed. p-value = 0.0080. IF staining of representative infrarenal vena cava images, including clots in the control and experimental groups and stained with anti-CD31, and Alexa Fluro secondary antibodies. 400x magnification is shown. Scale bars = 100 µm. Error bars refer to the SEM. Please click here to view a larger version of this figure.

Copyright © 2024 JoVE Journal of Visualized Experiments

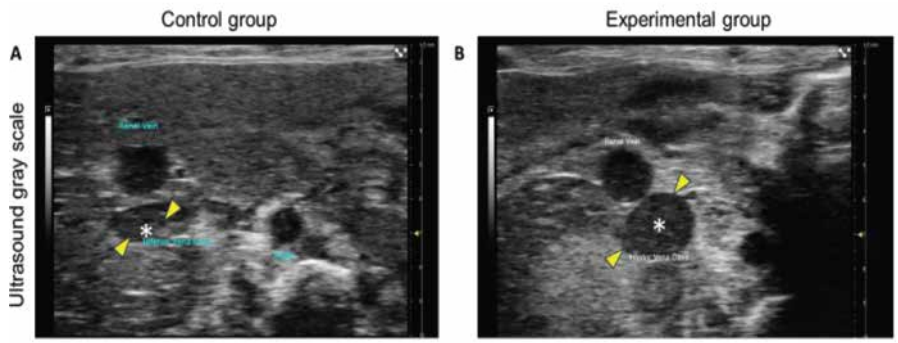

Figure 5: Increased clot surface area within the partially clamped IVC in group of mice with vascular clips IVC ligation. The Representative grayscale sonography images of the control and experimental group. (**A**) Representative grayscale Doppler image of the control group: A region of IVC shows an anechoic region suggestive of the patent lumen, and the other part shows a hyperechoic region indicative of the clot. (**B**) Representative grayscale Doppler image of the experimental group: The organized clot (white asterisk) within the IVC, as depicted with yellow arrowheads, was more prominent in the experimental group. Moreover, the clot appeared in two distinct manners in the sagittal section. A clot occluding the significant cross-section of the lumen was also delineated on the other side of IVC. Please click here to view a larger version of this figure.

Discussion

In a syngeneic xenograft colon cancer model, we observe higher thrombogenicity and expressions of coagulation markers in the experimental group compared to the control group. Importantly, the variance in all these parameters was lower in the experimental group compared to the control group. The modification involved introducing a vascular clip with a specific pressure profile at the confluence point of the IVC and the left renal vein. The clip was placed over a spacer, which was a 5-0 polypropylene suture. This modification reduces the variability in clot size and thrombosis markers. All mice experienced 100% survival.

Technical nuances

The procedure involved specific attention to several steps. Following laparotomy, both ureters were thoroughly inspected to prevent any accidental injury. To achieve optimal exposure, the intestines were covered in moist gauze and kept in the right upper quadrant without excessive traction. Next, the IVC side branches were cauterized 2 to 3 mm away from the ureters, IVC, and aorta to prevent damage to veins. After ensuring complete hemostasis, the plane for IVC ligation was prepared. It is important to note that the aorta and IVC in mice are closely connected along their course, and attempting to dissect them can lead to bleeding and loss of the animal. The only exception is the left renal vein and aorta confluence point[21]. A suture passage was then prepared using no more than three meticulous, sharp divergent movements with forceps.

The IVC diameter of an 8- to 12-week-old mouse is reported to be in the range of approximately 0.3 to 0.5 mm. The partial

IVC ligation procedure should secure space to differentiate from complete ligation. In the current study, we considered a 5-0 suture caliber, corresponding to 0.10 to 0.15 mm for the spacer. Therefore, the vascular clips lip space was adjusted for a 2-0 suture to provide adequate space for a 0.3 mm IVC and a 0.1 mm space.

The polypropylene suture provided a bloodless guide, allowing for the plane to be widened with repetitive caudal to the cranial movement for an additional 1 to 2 mm to accommodate the application of the vascular clips. Finally, the customized vascular clips with a lip remaining space compatible with a 5-0 polypropylene suture were placed.

The choice for noble metal clips, such as platinum, for blood vessel closure, is driven by the fact that such material is relatively inert and reduces material-induced inflammation compared to specific absorbable and delayed absorbable sutures[22,23,24]. These metal clips are resistant to chemical reactions, making them stable. This leads to a safer and more effective alternative with a lower risk of inflammation compared to the use of suture materials.

Translational relevance of the model

The murine venous thrombosis models are fundamentally different from deep vein thrombosis in humans. First, in rodent models, the clot formation is observed in the upstream direction. However, clinical VTs are formed downstream from a nidus[25,26]. Second, the cause-and-effect relationships are different between humans and mouse models. In humans, clot formation is the index event followed by blood flow obstruction. One exception is May-Thurner syndrome. May-Thurner syndrome refers to a medical condition in which increased external pressure on the left iliac vein, located between the spinal column and the right iliac artery, raises the risk of left iliac vein thrombosis, or a blood clot in the left iliac vein. In mouse models, the obstruction to venous flow is the primary event, which results in sluggish blood flow and thrombus formation[25].

Compared to other models, such as the femoral vein electrolytic injury model[12], IVC stasis offer a clear advantage. It allows examination of local therapeutic measures, such as IVC filters, catheter-directed thrombolysis and endoluminal recanalization with providing an environment for clot formation in the presence of blood flow. Thereby, two arms of the endothelial injury and stasis are examined in this model. Clots in IVC are also associated with higher occurrence of complications, such as pulmonary emboli. One limitation is that IVC is a less common site for DVT in humans.

Reduction-Refinement-Replacement (3R) framework

It is important to integrate the 3Rs framework in animal models. The integration of the 3R framework limits animal suffering and promotes ethical and responsible animal research practices. The 3Rs applies to our current finding since we observed no mortality in mice. Also, it is possible to use fewer animals in studies. Thus, the number of mice and the cost can be reduced.

Study limitations

A possible limitation of the clip method includes a relatively narrow pressure profile range of the tested vascular clips. Accordingly, further studies with a wide range of pressure profiles might be designed. Previous studies have shown that immunocompromised strain mice are more susceptible to clot formation, and the clot weights might differ in immunocompetent mice[12]. Future studies are encouraged to examine the extent of consistency of clot weights in different mouse strain backgrounds.

Conclusion

The current method provides a more consistent measure for venous thrombosis study via a partial IVC ligation model. We hope that this modification will allow the generation of robust and reliable murine models to investigate the consequences of cancer-associated thrombosis using different cancer models with relevance to human disease.

While the current work specifically focused on cancer-associated thrombosis, the future work will entail performing a comprehensive analysis of mouse models of different comorbidities (such as obesity, chronic kidney failure) and normal mice augmenting the risk of thrombosis.

Disclosures

The authors have nothing to disclose.

Acknowledgments

This work was supported by AHA Cardio-oncology SFRN CAT-HD Center grant 857078 (KR, VCC, XY, and SL) and R01HL166608 (KR and VCC).

References

1. Blom, J. W. et al. Incidence of venous thrombosis in a large cohort of 66,329 cancer patients: results of a record linkage study. *Journal of Thrombosis and Haemostasis.* **4** (3), 529-535 (2006).
2. Gabre, J. et al. Activated protein C accelerates venous thrombus resolution through heme oxygenase-1 induction. *Journal of Thrombosis and Haemostasis.* **12** (1), 93-102 (2014).
3. Chang, Y. S. et al. Sorafenib (BAY 43-9006) inhibits tumor growth and vascularization and induces tumor apoptosis and hypoxia in RCC xenograft models. *Cancer Chemotherapy and Pharmacology.* **59** (5), 561-574 (2007).
4. Khorana, A. A., Kuderer, N. M., Culakova, E., Lyman, G. H., Francis, C. W. Development and validation of a predictive model for chemotherapy-associated thrombosis. *Blood.* **111** (10), 4902-4907 (2008).
5. Chew, H. K., Wun, T., Harvey, D., Zhou, H., White, R.H. Incidence of venous thromboembolism and its effect on survival among patients with common cancers. *Archives of Internal Medicine.* **166** (4), 458-464 (2006).
6. Leiva, O., Newcomb, R., Connors, J. M., Al-Samkari, H. Cancer and thrombosis: new insights to an old problem. *Journal de Medecine Vasculaire.* **45** (6S), 6S8-6S16 (2020).
7. Chen, N. et al. Bevacizumab promotes venous thromboembolism through the induction of PAI-1 in a mouse xenograft model of human lung carcinoma. *Molecular Cancer.* **14**, 140 (2015).
8. Goto, H. et al. Activity of a new vascular targeting agent, ZD6126, in pulmonary metastases by human lung adenocarcinoma in nude mice. *Cancer Research.* **62** (13), 3711-3715 (2002).
9. Jiang, Y. et al. Inhibition of anchorage-independent growth and lung metastasis of A549 lung carcinoma cells by IkappaBbeta. *Oncogene.* **20** (18), 2254-2263 (2001).
10. Salup, R. R., Wiltrout, R. H. Adjuvant immunotherapy of established murine renal cancer by interleukin 2-stimulated cytotoxic lymphocytes. *Cancer Research.* **46** (7), 3358-3363 (1986).
11. Deatrick, K. B. et al. The effect of matrix metalloproteinase 2 and matrix metalloproteinase 2/9 deletion in experimental post-thrombotic vein wall

remodeling. *Journal of Vascular Surgery.* **58** (5), 1375-1384.e2 (2013).

12. Diaz, J. A. et al. Choosing a mouse model of venous thrombosis: a consensus assessment of utility and application. *Journal of Thrombosis and Haemostasis.* **17** (4), 699-707 (2019).
13. Henke, P. K. et al. Toll-like receptor 9 signaling is critical for early experimental deep vein thrombosis resolution. *Arteriosclerosis, Thrombosis, and Vascular Biology.* **31** (1), 43-49 (2011).
14. Liu, H. et al. Inferior vena cava stenosis-induced deep vein thrombosis is influenced by multiple factors in rats. *Biomedicine & Pharmacotherapy.* **128**, 110270 (2020).
15. von Brühl, M. L. et al. Monocytes, neutrophils, and platelets cooperate to initiate and propagate venous thrombosis in mice in vivo. *The Journal of Experimental Medicine.* **209** (4), 819-835 (2012).
16. Brill, A. et al. von Willebrand factor-mediated platelet adhesion is critical for deep vein thrombosis in mouse models. *Blood.* **117** (4), 1400-1407 (2011).
17. Stark, K. et al. Distinct Pathogenesis of Pancreatic Cancer Microvesicle-Associated Venous Thrombosis Identifies New Antithrombotic Targets In Vivo. *Arteriosclerosis, Thrombosis, and Vascular Biology.* **38** (4), 772-786 (2018).
18. Belghasem, M. et al. Metabolites in a mouse cancer model enhance venous thrombogenicity through the aryl hydrocarbon receptor-tissue factor axis. *Blood.* **134** (26), 2399-2413 (2019).
19. Tracz, A., Mastri, M., Lee, C. R., Pili, R., Ebos, J. M. Modeling spontaneous metastatic renal cell carcinoma (mRCC) in mice following nephrectomy. *Journal of Visualized Experiments.* (86), e51485 (2014).
20. Lertkiatmongkol, P., Liao, D., Mei, H., Hu, Y., Newman, P. J. Endothelial functions of platelet/endothelial cell adhesion molecule-1 (CD31). *Current Opinion in Hematology.* **23** (3), 253-259 (2016).
21. Payne, H., Brill, A. Stenosis of the Inferior Vena Cava: A Murine Model of Deep Vein Thrombosis. *Journal of Visualized Experiments.* (130), e56697 (2017).
22. Yabit, F., Hughes, L., Sylvester, B., Tiesenga, F. Hypersensitivity Reaction Post Laparoscopic Cholecystectomy Due to Retained Titanium Clips. *Cureus.* **14** (6), e26167 (2022).
23. Nagorni, E. A. et al. Post-laparoscopic cholecystectomy Mirizzi syndrome induced by polymeric surgical clips: a case report and review of the literature. *Journal of Medical Case Reports.* **10**, 135 (2016).
24. Zemelka-Wiacek, M. Metal Allergy: State-of-the-Art Mechanisms, Biomarkers, Hypersensitivity to Implants. *Journal of Clinical Medicine.* **11** (23), 6971 (2022).
25. Poyyamoli, S. et al. May-Thurner syndrome. *Cardiovascular Diagnosis and Therapy.* **11** (5), 1104-1111 (2021).
26. Streiff, M. B. et al. NCCN Guidelines Insights: Cancer-Associated Venous Thromboembolic Disease, Version 2.2018. *Journal of the National Comprehensive Cancer Network.* **16** (11), 1289-1303 (2018).

Copyright © 2024 JoVE Journal of Visualized Experiments